Understanding Doping, Vacancy, Lattice Stability, and Superconductivity in $K_xFe_{2-y}Se_2$

Yu Liu, Gang Wang, Tianping Ying, Xiaofang Lai, Shifeng Jin, Ning Liu, Jiangping Hu, and Xiaolong Chen**

The discovery of superconductivity in $A_xFe_{2-y}Se_2$ (A = K, Cs, Rb, Tl/Rb, Tl/K)[1–6] triggered another surge of research on iron-based superconductors, which were previously only featured by iron pnictides[7–12] and β-FeSe.[13] The new series of superconductors can be regarded as the formation from the intercalation of metals between the FeSe layers of β-FeSe. In comparison to the iron pnictides, metal-intercalated iron selenides are much more complicated in terms of structure, chemical composition, and phases. The nature of the superconducting (SC) phase, for example, is still in debate though considerable progress has been made over the last few years.[14–16]

One of the most controversial issues is whether the SC phase is Fe vacancy free or not, i.e., the FeSe layers in $A_xFe_{2-y}Se_2$ are stoichiometric ($y = 0$), or off-stoichiometric due to the existence of considerable Fe vacancies. The origin of this issue is largely due to the phase separation that inevitably occurs in these systems at 500–578 K,[17] leading to the coexistence of the insulating phase ($A_2Fe_4Se_5$) and the SC phase.[18–23] The thus-obtained SC phase is not standing freely; instead, it intergrows with the insulating phase in the form of nanostrip and its volume fraction is quite low, 10%–20%, as estimated by various measurements.[24–29] This is the main obstacle that prohibits the precise determination of the structure and the composition of the SC phase. Ying et al.[30,31] verified that the SC phases in the K-intercalated iron selenides are almost no Fe vacancy in the FeSe layers based on their study of the superconductors obtained via a liquid ammonia route. The neutron diffraction showed that the 43 K SC phase in Li/ammonia co-intercalated FeSe compound is Fe vacancy free in a separate study.[32] Guo et al.[33] synthesized a 37 K SC phase containing slight Fe vacancy by the similar liquid ammonia method. In the $K_xFe_{2-y}Se_2$ film grown on $SrTiO_3$ (001) substrate, an Fe-vacancy-free phase KFe_2Se_2 with $\sqrt{2} \times \sqrt{5}$ charge ordering was observed in the SC region.[34,35] Different opinions, however, exist. For example, the SC phases are thought to originate from superstructures due to Fe vacancy, such as 2×4[36] or $\sqrt{8} \times \sqrt{10}$.[37] Meanwhile, phases with disordered Fe vacancies were also reported to be SC.[38,39] Apart from Fe vacancies, the possibility of the existence of about 20% excess Fe in an SC phase with transition temperature (T_c) of 44 K in the K-Fe-Se system was also reported.[40]

Another puzzling issue is the existence of several SC phases with different T_c from 30 to 46 K, which are often mixed in a single sample. For instance, apart from a dominated 30 K phase, a 44 K phase of trace amount sometimes can be observed in a $K_xFe_{2-y}Se_2$ sample obtained by a high-temperature route.[41] The amount of 44 K phase can be enhanced in samples with a little less K content ($x = 0.6$–0.7), but its real compositions are unknown. The results in ref.[31] revealed that the obtained SC phases differ only in K contents, $K_{0.3}Fe_2Se_2$ with a $T_c = 44$ K and $K_{0.6}Fe_2Se_2$ with a $T_c = 30$ K. Superconductivity with T_c of 30 K and 43 K was also observed in $K_xFe_{2-y}Se_2$ samples with $\sqrt{2} \times \sqrt{2} \times 1$ superstructure due to K vacancy ordering, but the phases for different T_c have not been specified.[25,28,42,43] In addition, K-intercalated iron selenide with excess Fe was also proposed to have T_c of 44 K.[40]

So far, there has been no consensus on the answers to the above issues. Moreover, the underlying mechanism of the lattice stability and vacancy is also poorly understood, in particular, in terms of the origin for multifarious structures. To address these issues, here, we first study the energetic change and structural evolution as a function of intercalated metal content by taking $K_xFe_{2-y}Se_2$ as an example using first-principles calculations. Two competing factors are found to dominate the formation of the phases and the structural evolution. One is due to the energy increase caused by the accumulation of the negative charge in FeSe layers. The other is due to the Coulomb attraction between the K ion layers and the negatively charged FeSe layers. Then we show that the intercalated K content at $0.25 \le x \le 0.6$ can stabilize the body centered tetragonal (bct) lattice and Fe is favored to fully occupy its site. At $x > 0.6$, the structure is stabilized by creating Fe vacancies in FeSe layers. At low intercalated K level, $x < 0.25$, the structure will collapse due to the lattice instability. Then a schematic phase diagram is constructed accordingly whereby we speculate the SC phases are $K_xFe_{2-y}Se_2$ with $0.25 \le x \le 0.6$ and $y = 0$. Our finding sheds

Dr. Y. Liu, Prof. G. Wang, Dr. T. Ying, Dr. X. Lai, Dr. S. Jin, N. Liu, Prof. X. Chen
Research and Development Center for Functional Crystals
Beijing National Laboratory for Condensed Matter Physics
Institute of Physics
Chinese Academy of Sciences
Beijing 100190, P.R. China
E-mail: gangwang@iphy.ac.cn; chenx29@iphy.ac.cn
Prof. J. Hu
Beijing National Laboratory for Condensed Matter Physics
Institute of Physics
Chinese Academy of Sciences
Beijing 100190, P.R. China
Prof. J. Hu, Prof. X. Chen
Collaborative Innovation Center of Quantum Matter
Beijing, P.R. China

DOI: 10.1002/advs.201600098

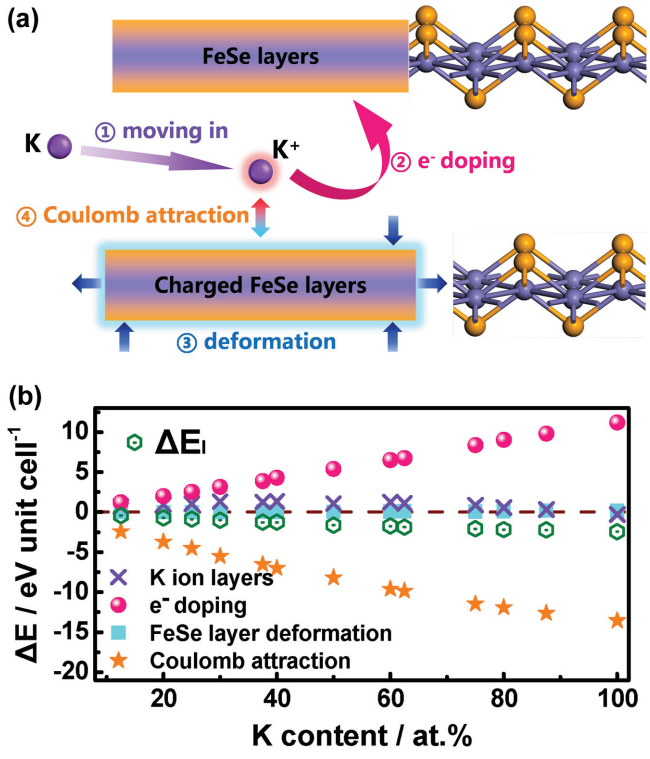

Figure 1. a) The schematic of the K intercalation process. It does not represent a certain structure. b) The total formation energy and the energy change due to the formation of K ion layers, the electron doping in FeSe layers, the deformation of FeSe layers, and the Coulomb attraction between K ion layers and FeSe layers as a function of the K content, respectively.

some light on understanding this distinct SC family and should also be applicable to other metal-intercalated iron selenides besides $K_xFe_{2-y}Se_2$.

To begin with, we study the formation energy for the process of K intercalation. The process can be expressed as a chemical reaction

$$x\mathrm{K} + 2\mathrm{FeSe} \rightarrow \mathrm{K}_x\mathrm{Fe}_2\mathrm{Se}_2\,(0 < x \leq 1)$$

The formation energy per unit cell can be described as $\Delta E_I = E_{K_xFe_2Se_2} - E_{K_0Fe_2Se_2} - xE_K$, where $E_{K_xFe_2Se_2}$ and $E_{K_0Fe_2Se_2}$ are the total energies of $K_xFe_2Se_2$ and an assumed $K_0Fe_2Se_2$ with a similar bct structure but without any K ion, and E_K is the energy of elemental K. The variation of ΔE_I versus K content is shown in **Figure 1**, which indicates that the intercalation of K into FeSe layers is always energetically favored for the bct structure.

Then we break down ΔE_I in terms of energy from the structural constituent units and their interactions. For the K intercalation process, as shown in Figure 1a, K atoms lose their valence electrons and form K ion layers between adjacent FeSe layers after K entering into the lattice, while FeSe layers are charged and deformed and eventually lead to $K_xFe_2Se_2$ with a bct structure. Hence, the following contributions to the total formation energy are considered:

(1) The formation of K ion layers: $\Delta E_{\text{K ion layers}} = E_{(\text{K ion layers})x+} - xE_K$

(2) The electron doping in FeSe layers: $\Delta E_{\text{e- doping}} = E_{(\text{FeSe layers})x-} - E_{\text{FeSe layers}}$

(3) The deformation of FeSe layers: $\Delta E_{\text{FeSe layer deformation}} = E_{\text{FeSe layers}} - E_{\text{K0Fe2Se2}}$

(4) The Coulomb attraction between K ion layers and FeSe layers: $\Delta E_C = E_{K_xFe_2Se_2} - E_{(\text{FeSe layers})x-} - E_{(\text{K ion layers})x+}$

And $E_{(\text{K ion layers})x+}$ is the energy of K ion layers, $E_{(\text{FeSe layers})x-}$ the energy of charged FeSe layers, and $E_{\text{FeSe layers}}$ the energy of FeSe layers in $K_xFe_2Se_2$. Therefore, the total formation energy can be written as the sum of these four energy changes: $\Delta E_I = \Delta E_{\text{K ion layers}} + \Delta E_{\text{e-doping}} + \Delta E_{\text{FeSe layer deformation}} + \Delta E_C$.

The variations of these four energy contributions as a function of the K content are calculated and the results are shown in Figure 1b, respectively. First of all, FeSe layers are prominent in contributing more and more positive energy to ΔE_I when they are negatively charged with more and more electrons. This is easily understood since charging a neutral FeSe sheet will incur additional energy like charging a capacitor. Inversely, with the increasing K content, more charges will come into effect in the Coulomb attraction between K ion layers and the charged FeSe layers and thus greatly enhance $|\Delta E_C|$, which will sufficiently offset the increase of energy induced by electron doping into the FeSe layer. In contrast with these two contributions, the other two energy contributions due to the formation of K ion layers and the deformation of FeSe layers are much smaller. Therefore, we conclude that the former two contributions dominate the energy change during the K intercalation.

To understand the tendency for appearance of Fe vacancy in the K-intercalated iron selenides, we go further to consider the energy change $\Delta E_{\text{Fe vacancy}}$ ($= \Delta E_I' - \Delta E_I - \mu_{Fe}$, where $\Delta E_I' = E_{K_xFe_{1.94}Se_2} - E_{K_0Fe_{1.94}Se_2} - xE_K$ is the formation energy per unit cell in the Fe deficiency structure and μ_{Fe} is the Fe chemical potential.) by removal of an Fe atom from the unit lattice of $K_xFe_2Se_2$ and its dependence on the K content. It is found that $\Delta E_{\text{Fe vacancy}}$ only fluctuates above and below zero when $x \leq 0.6$ as shown in **Figure 2**a. When $x > 0.6$, $\Delta E_{\text{Fe vacancy}}$ rapidly drops, revealing that Fe vacancies are favored at high levels of K intercalation. This is easily understood since K has a smaller electronegativity than Fe, when the doped electrons due to K are over a limit that Fe—Se bond can accommodate, the surplus electrons will prefer to transfer into Fe^{2+}. In this way, Fe is repelled out of the lattice in the form of an element. The final compound with Fe vacancy is more energetically a favored state. The limit is around at $x = 0.6$. The $K_2Fe_4Se_5$ phase contains 20% Fe vacancy corresponding to $x = 0.8$ is a manifestation of this argument. This tendency of appearance of Fe vacancy with K content is supported by the experimental results.[30–32]

Besides the above considerations on the formation energy, the influence of lattice dynamics on the structural stability should also be accounted for. This is, in particular, true for the compounds with low levels of intercalated K, which can induce lattice instability. Figure 2b shows the density of phonon states (DOPS) of $K_{0.2}Fe_2Se_2$, where negative frequencies appear, meaning the structure is unstable. Partial DOPS further indicate that it is mainly because of the considerable amount of highly unstable Se atoms, which are unbonded due to the

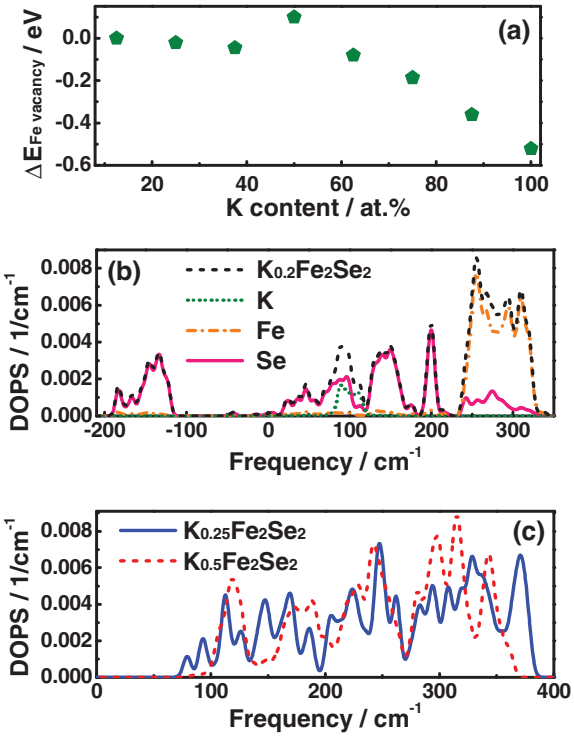

Figure 2. a) The relative variation of formation energy change between $K_xFe_{1.94}Se_2$ and $K_xFe_2Se_2$ as a function of the K content. As the absolute value will be determined by Fe chemical potential ($\Delta E_{Fe\ vacancy} = \Delta E_l' - \Delta E_l - \mu_{Fe}$), the change of formation energy between $K_{0.125}Fe_{1.94}Se_2$ and $K_{0.125}Fe_2Se_2$ is set to zero to show the relative values for comparison. b) Total and partial DOPS of $K_{0.2}Fe_2Se_2$. c) DOPS of $K_{0.25}Fe_2Se_2$ and $K_{0.5}Fe_2Se_2$.

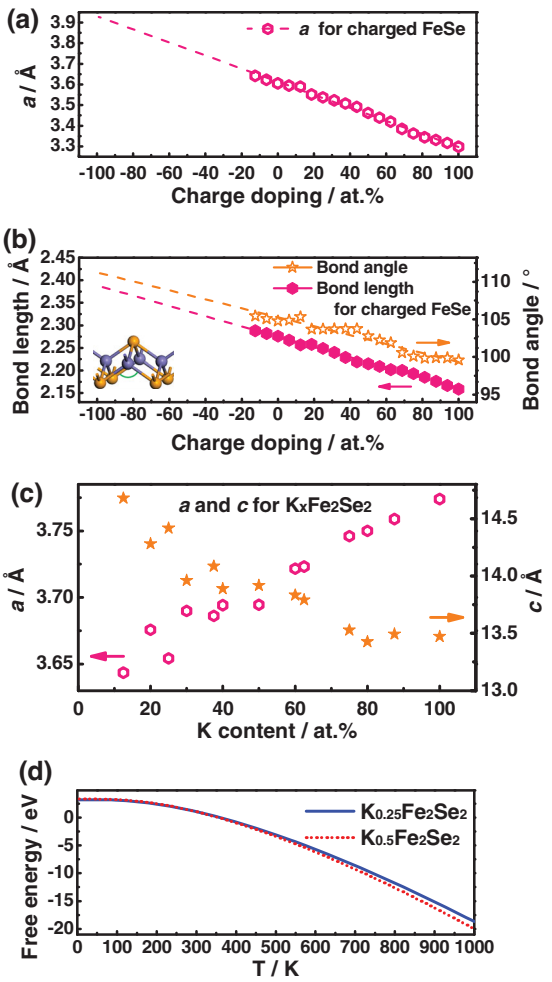

Figure 3. a) The lattice constant *a*, b) the Fe—Se bond length and the Se—Fe—Se bond angle (see details in the inset) along FeSe layers as a function of charge per unit cell. Positive charge means hole-doped and negative one being electron-doped. Dashed lines represent the results of linear fitting. c) The variation of the lattice constants *a* (pink rings) and *c* (orange stars) with the K content in $K_xFe_2Se_2$. d) The free energy of $K_{0.25}Fe_2Se_2$ and $K_{0.5}Fe_2Se_2$ as a function of temperature.

absence of K nearby. The phonon density, however, exhibits no imaginary mode for all other compounds with $x \geq 0.25$. As examples, Figure 2c shows the DOPS for $K_{0.25}Fe_2Se_2$ and $K_{0.5}Fe_2Se_2$. The above results demonstrate that the phases of $K_xFe_2Se_2$ free of Fe vacancy are both energetically and dynamically favored in the K intercalation range of $0.25 \leq x \leq 0.6$.

Now we are focused on the trend of structural change upon K intercalation in the range of $0.25 \leq x \leq 0.6$. Both electronic and size effects of K will be taken into account. In order to better understand the role of electron doping in the structural change, we charge $K_0Fe_2Se_2$ with various electron concentrations, which allows us to explore the effect of electron doping while excluding the size influence of K. As shown in **Figure 3**a,b, the changes in the lattice constant *a*, the Fe—Se bond, and the Se—Fe—Se angle clearly indicate that FeSe layers are stretched along the *ab* plane upon electron doping alone. (Note the results of the highly electron-doped are extrapolated from the trend of the positively charged ones simply because the stable negatively charged $K_0Fe_2Se_2$ cannot always be obtained during the iterative calculations.) For a more realistic case, other factors such as the lattice mismatch and the Coulomb attraction must be included. Figure 3c shows the lattice parameter variations with K intercalation, which accounts for all these contributions together with the electron doping. We see that the overall effect of K intercalation increases the lattice constant *a*, stretches FeSe layers, and reduces the lattice constant *c*. For instance, the lattice constant *a* of $K_{0.25}Fe_2Se_2$ and $K_{0.5}Fe_2Se_2$ expands from 3.65 Å to 3.69 Å and *c* shrinks from 14.42 Å to 13.92 Å. The predicted lattice constant *c* of $K_{0.25}Fe_2Se_2$, 14.42 Å agrees with 14.28(4) Å of $K_{0.3}Fe_2Se_2$ having T_c of 44 K.[31] And the predicted lattice constants *a* and *c* for $K_{0.5}Fe_2Se_2$, 3.69 Å and 13.92 Å are consistent with the periods observed using scanning tunneling microscope along [110] and [001], 5.5 Å ($\sqrt{2}a$) and 14.1 Å,[26] respectively, considering the calculation accuracy. It is worth noting that a similar trend of the changes in lattice parameters was observed in other electron-doped $ThCr_2Si_2$ structures, such as KFe_2As_2[9,44] and $CaFe_2As_2$.[45]

Furthermore, we explore the temperature-dependent stability of structures in the K region of interest. To this end, we perform the molecular dynamics (MD) simulations on $K_{0.25}Fe_2Se_2$ and $K_{0.5}Fe_2Se_2$. Both structures can survive for at least 1 picosecond using $2\sqrt{2} \times 2\sqrt{2} \times 1$ super cells at temperatures up to 500 K, indicating that they are stable at these temperatures.[46] It should be worth noting that the atom displacements of

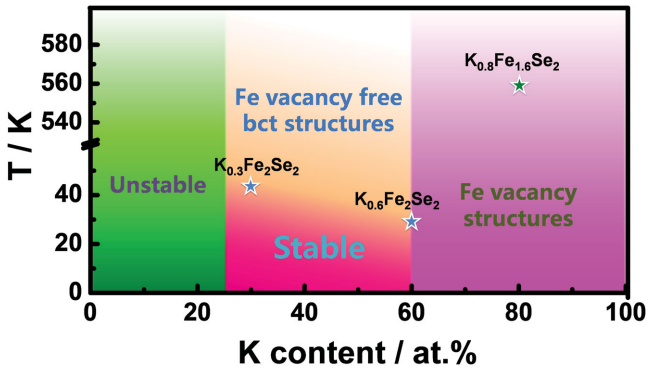

Figure 4. Schematic phase diagram of $K_xFe_{2-y}Se_2$.

$K_{0.25}Fe_2Se_2$ are larger than those of $K_{0.5}Fe_2Se_2$, suggesting that $K_{0.25}Fe_2Se_2$ is less stable. The variations of free energy with temperature for the two phases are also calculated and shown in Figure 3d. The free energy is more favorable for $K_{0.5}Fe_2Se_2$ at temperatures above 268 K, consistent with the result obtained by MD. Despite their variations in stability, both of them have the electronic structures similar to KFe_2Se_2 (see Figure S3, Supporting Information), which suggests that they should have similar properties to KFe_2Se_2. Considering stoichiometry, formation energy, stability, and electronic structures, $K_{0.25}Fe_2Se_2$ and $K_{0.5}Fe_2Se_2$ (see Figure S2, Supporting Information for their structures) are proposed to be responsible for the observed superconductivity at 44 and 30 K,[31] respectively. The relative stability difference could also explain the difficulty to obtain the 44 K phase.

Based on the results presented above, we schematize a phase diagram for the $K_xFe_{2-y}Se_2$ system in **Figure 4**. In the K-rich portion with $x > 0.6$, phases with Fe vacancies tend to exist, agreeing well with the observed antiferromagnetic $K_2Fe_4Se_5$ phase. As for the low level K-intercalated compounds ($x < 0.25$), there has been no report on the synthesis of free-standing $K_xFe_2Se_2$. We note that the two identified SC phases $K_{0.3}Fe_2Se_2$ and $K_{0.6}Fe_2Se_2$ lie in the region of $0.25 \le x \le 0.6$.[31] T_c is 44 K for the former phase and 30 K for the latter one, suggesting that T_c is dependent on the K content or the doped electron concentrations. Although experimentally observed K contents in SC phases by far are discrete, recent reports about carrier concentration tuning of T_c from 30 to above 40 K in FeSe thin flakes[47,48] implies that their variation of T_c with carrier concentration can be continuous, similar to the cases in other high-temperature superconductors. Further improvement of T_c can be expected considering the experimental progresses achieved in single-layer FeSe films.[49–54] Therefore, we infer that the 30 K phase is electron overdoped and the 44 K phase also might not be optimally tuned. Moreover, in alkali-metal-intercalated FeSe compounds prepared at low temperatures, the synergic effect of NH_3, NH_2, or $C_2H_4(NH_2)_2$ along with alkali metal can stabilize the structures.[31,32,55] These offer us an effective strategy to raise T_c of bulk iron-selenide-based superconductors by controlling carrier doping while stabilizing the structures by intercalations or effect of substrates. At the moment, tremendous efforts are needed toward this goal. Because of the calculation limit and accuracy, we do not consider the slight off-stoichiometric cases, say, the Fe vacancy concentration is less than 3 at%. It should be pointed out that such slight off-stoichiometry is tolerated in $K_xFe_2Se_2$ just like many other materials which may be the reason that superconductivity was observed in previous reports of refs. [33,40].

In conclusion, we carefully investigate the energetic change and structural evolution of $K_xFe_{2-y}Se_2$ as a function of intercalated K content using first-principles calculations. Two factors dominating the formation of the phases and the structural evolution are confirmed. One is due to the accumulation of negative charge in FeSe layers, the other is due to Coulomb attraction between K ion layers and negatively charged FeSe layers. The structural evolution of this series of phases is summarized: at $0.25 \le x \le 0.6$, the bct lattice is stable and Fe is favored to full occupy its site; at $x > 0.6$, FeSe layers tend to exclude Fe atoms and create Fe vacancies; and at $x < 0.25$, the structure will collapse for the dynamic instability. A schematic phase diagram is constructed accordingly and the possible route to further improve T_c is suggested. The phases responding to the observed superconductivity are proposed to be $K_{0.25}Fe_2Se_2$ and $K_{0.5}Fe_2Se_2$ in terms of stoichiometry, formation energy, stability, and electronic structures. Though based on the study of $K_xFe_{2-y}Se_2$, our results should be meaningful to understand the SC and its related phases in metal-intercalated iron selenides and other similar SC systems.

Supporting Information

Supporting Information is available from the Wiley Online Library or from the author.

Acknowledgements

Y. Liu would like to thank S. J. Shen of Institute of Physics, Chinese Academy of Sciences, for the fruitful discussions. This work was partly supported by the National Natural Science Foundation of China (Grant Nos. 51322211, 91422303, and 51532010), the Strategic Priority Research Program (B) of the Chinese Academy of Sciences (Grant No. XDB07020100), Ministry of Education of China (2012 Academic Scholarship Award for Doctoral Candidates), the International Centre for Diffraction Data (2013 Ludo Frevel Crystallography Scholarship Award), and K. C. Wong Education Foundation, Hong Kong.

Received: March 15, 2016
Revised: April 19, 2016
Published online: May 17, 2016

[1] J. G. Guo, S. F. Jin, G. Wang, S. C. Wang, K. X. Zhu, T. T. Zhou, M. He, X. L. Chen, *Phys. Rev. B* **2010**, *82*, 180520.
[2] A. Krzton-Maziopa, Z. Shermadini, E. Pomjakushina, V. Pomjakushin, M. Bendele, A. Amato, R. Khasanov, H. Luetkens, K. Conder, *J. Phys. Condens. Mat.* **2011**, *23*, 052203.
[3] A. F. Wang, J. J. Ying, Y. J. Yan, R. H. Liu, X. G. Luo, Z. Y. Li, X. F. Wang, M. Zhang, G. J. Ye, P. Cheng, Z. J. Xiang, X. H. Chen, *Phys. Rev. B* **2011**, *83*, 060512.
[4] L. J. Zhang, D. J. Singh, *Phys. Rev. B* **2009**, *79*, 094528.
[5] H. D. Wang, C. H. Dong, Z. J. Li, Q. H. Mao, S. S. Zhu, C. M. Feng, H. Q. Yuan, M. H. Fang, *Europhys. Lett.* **2011**, *93*, 47004.
[6] M. H. Fang, H. D. Wang, C. H. Dong, Z. J. Li, C. M. Feng, J. Chen, H. Q. Yuan, *Europhys. Lett.* **2011**, *94*, 27009.

[7] Y. Kamihara, T. Watanabe, M. Hirano, H. Hosono, *J. Am. Chem. Soc.* **2008**, *130*, 3296.
[8] M. Rotter, M. Tegel, D. Johrendt, *Phys. Rev. Lett.* **2008**, *101*, 107006.
[9] K. Sasmal, B. Lv, B. Lorenz, A. M. Guloy, F. Chen, Y. Y. Xue, C. W. Chu, *Phys. Rev. Lett.* **2008**, *101*, 107007.
[10] J. H. Tapp, Z. Tang, B. Lv, K. Sasmal, B. Lorenz, P. C. W. Chu, A. M. Guloy, *Phys. Rev. B* **2008**, *78*, 060505.
[11] X. C. Wang, Q. Q. Liu, Y. X. Lv, W. B. Gao, L. X. Yang, R. C. Yu, F. Y. Li, C. Q. Jin, *Solid State Commun.* **2008**, *148*, 538.
[12] B. Lv, L. Deng, M. Gooch, F. Wei, Y. Sun, J. K. Meen, Y. Y. Xue, B. Lorenz, C. W. Chu, *Proc. Natl. Acad. Sci. USA* **2011**, *108*, 15705.
[13] F. C. Hsu, J. Y. Luo, K. W. Yeh, T. K. Chen, T. W. Huang, P. M. Wu, Y. C. Lee, Y. L. Huang, Y. Y. Chu, D. C. Yan, M. K. Wu, *Proc. Natl. Acad. Sci. USA* **2008**, *105*, 14262.
[14] Y. Zhang, L. X. Yang, M. Xu, Z. R. Ye, F. Chen, C. He, H. C. Xu, J. Jiang, B. P. Xie, J. J. Ying, X. F. Wang, X. H. Chen, J. P. Hu, M. Matsunami, S. Kimura, D. L. Feng, *Nat. Mater.* **2011**, *10*, 273.
[15] M. Y. Wang, C. Fang, D. X. Yao, G. T. Tan, L. W. Harriger, Y. Song, T. Netherton, C. L. Zhang, M. Wang, M. B. Stone, W. Tian, J. P. Hu, P. C. Dai, *Nat. Commun.* **2011**, *2*, 580.
[16] L. L. Sun, X. J. Chen, J. Guo, P. W. Gao, Q. Z. Huang, H. D. Wang, M. H. Fang, X. L. Chen, G. F. Chen, Q. Wu, C. Zhang, D. C. Gu, X. L. Dong, L. Wang, K. Yang, A. G. Li, X. Dai, H. K. Mao, Z. X. Zhao, *Nature* **2012**, *483*, 67.
[17] F. Ye, S. Chi, W. Bao, X. F. Wang, J. J. Ying, X. H. Chen, H. D. Wang, C. H. Dong, M. H. Fang, *Phys. Rev. Lett.* **2011**, *107*, 137003.
[18] W. Bao, Q. Z. Huang, G. F. Chen, M. A. Green, D. M. Wang, J. B. He, Y. M. Qiu, *Chin. Phys. Lett.* **2011**, *28*, 086104.
[19] Y. J. Yan, M. Zhang, A. F. Wang, J. J. Ying, Z. Y. Li, W. Qin, X. G. Luo, J. Q. Li, J. P. Hu, X. H. Chen, *Sci. Rep.* **2012**, *2*, 212.
[20] P. C. Dai, J. P. Hu, E. Dagotto, *Nat. Phys.* **2012**, *8*, 709.
[21] H. H. Wen, *Rep. Prog. Phys.* **2012**, *75*, 112501.
[22] D. P. Shoemaker, D. Y. Chung, H. Claus, M. C. Francisco, S. Avci, A. Llobet, M. G. Kanatzidis, *Phys. Rev. B* **2012**, *86*, 184511.
[23] E. Dagotto, *Rev. Mod. Phys.* **2013**, *85*, 849.
[24] F. Chen, M. Xu, Q. Q. Ge, Y. Zhang, Z. R. Ye, L. X. Yang, J. Jiang, B. P. Xie, R. C. Che, M. Zhang, A. F. Wang, X. H. Chen, D. W. Shen, J. P. Hu, D. L. Feng, *Phys. Rev. X* **2011**, *1*, 021020.
[25] R. H. Yuan, T. Dong, Y. J. Song, P. Zheng, G. F. Chen, J. P. Hu, J. Q. Li, N. L. Wang, *Sci. Rep.* **2012**, *2*, 221.
[26] W. Li, H. Ding, P. Deng, K. Chang, C. L. Song, K. He, L. L. Wang, X. C. Ma, J. P. Hu, X. Chen, Q. K. Xue, *Nat. Phys.* **2012**, *8*, 126.
[27] A. Charnukha, A. Cvitkovic, T. Prokscha, D. Propper, N. Ocelic, A. Suter, Z. Salman, E. Morenzoni, J. Deisenhofer, V. Tsurkan, A. Loidl, B. Keimer, A. V. Boris, *Phys. Rev. Lett.* **2012**, *109*, 017003.
[28] Z. W. Wang, Z. Wang, Y. J. Song, C. Ma, Y. Cai, Z. Chen, H. F. Tian, H. X. Yang, G. F. Chen, J. Q. Li, *J. Phys. Chem. C* **2012**, *116*, 17847.
[29] M. Bendele, A. Barinov, B. Joseph, D. Innocenti, A. Iadecola, A. Bianconi, H. Takeya, Y. Mizuguchi, Y. Takano, T. Noji, T. Hatakeda, Y. Koike, M. Horio, A. Fujimori, D. Ootsuki, T. Mizokawa, N. L. Saini, *Sci. Rep.* **2014**, *4*, 5592.
[30] T. P. Ying, X. L. Chen, G. Wang, S. F. Jin, T. T. Zhou, X. F. Lai, H. Zhang, W. Y. Wang, *Sci. Rep.* **2012**, *2*, 426.
[31] T. P. Ying, X. L. Chen, G. Wang, S. F. Jin, X. F. Lai, T. T. Zhou, H. Zhang, S. J. Shen, W. Y. Wang, *J. Am. Chem. Soc.* **2013**, *135*, 2951.
[32] M. Burrard-Lucas, D. G. Free, S. J. Sedlmaier, J. D. Wright, S. J. Cassidy, Y. Hara, A. J. Corkett, T. Lancaster, P. J. Baker, S. J. Blundell, S. J. Clarke, *Nat. Mater.* **2013**, *12*, 15.
[33] J. G. Guo, H. C. Lei, F. Hayashi, H. Hosono, *Nat. Commun.* **2014**, *5*, 4756.
[34] W. Li, H. Ding, Z. Li, P. Deng, K. Chang, K. He, S. H. Ji, L. L. Wang, X. C. Ma, J. P. Hu, X. Chen, Q. K. Xue, *Phys. Rev. Lett.* **2012**, *109*, 057003.
[35] L. L. Wang, X. C. Ma, X. Chen, Q. K. Xue, *Chin. Phys. B* **2013**, *22*, 086801.
[36] J. Zhao, H. B. Cao, E. Bourret-Courchesne, D. H. Lee, R. J. Birgeneau, *Phys. Rev. Lett.* **2012**, *109*, 267003.
[37] X. X. Ding, D. L. Fang, Z. Y. Wang, H. Yang, J. Z. Liu, Q. Deng, G. B. Ma, C. Meng, Y. H. Hu, H. H. Wen, *Nat. Commun.* **2013**, *4*, 1897.
[38] Z. Wang, Y. J. Song, H. L. Shi, Z. W. Wang, Z. Chen, H. F. Tian, G. F. Chen, J. G. Guo, H. X. Yang, J. Q. Li, *Phys. Rev. B* **2011**, *83*, 140505.
[39] T. Berlijn, P. J. Hirschfeld, W. Ku, *Phys. Rev. Lett.* **2012**, *109*, 147003.
[40] A. M. Zhang, T. L. Xia, K. Liu, W. Tong, Z. R. Yang, Q. M. Zhang, *Sci. Rep.* **2013**, *3*, 1216.
[41] D. M. Wang, J. B. He, T. L. Xia, G. F. Chen, *Phys. Rev. B* **2011**, *83*, 132502.
[42] A. Ricci, B. Joseph, N. Poccia, G. Campi, N. Saini, A. Bianconi, *J. Supercond. Nov. Magn.* **2014**, *27*, 1003.
[43] Z. Wang, Y. Cai, Z. W. Wang, C. Ma, Z. Chen, H. X. Yang, H. F. Tian, J. Q. Li, *Phys. Rev. B* **2015**, *91*, 064513.
[44] M. Rotter, M. Pangerl, M. Tegel, D. Johrendt, *Angew. Chem. Int. Ed.* **2008**, *47*, 7949.
[45] S. R. Saha, N. P. Butch, T. Drye, J. Magill, S. Ziemak, K. Kirshenbaum, P. Y. Zavalij, J. W. Lynn, J. Paglione, *Phys. Rev. B* **2012**, *85*, 024525.
[46] Y. Liu, G. Wang, Q. S. Huang, L. W. Guo, X. L. Chen, *Phys. Rev. Lett.* **2012**, *108*, 225505.
[47] B. Lei, J. H. Cui, Z. J. Xiang, C. Shang, N. Z. Wang, G. J. Ye, X. G. Luo, T. Wu, Z. Sun, X. H. Chen, *Phys. Rev. Lett.* **2016**, *116*, 077002.
[48] B. Lei, Z. J. Xiang, X. F. Lu, N. Z. Wang, J. R. Chang, C. Shang, A. M. Zhang, Q. M. Zhang, X. G. Luo, T. Wu, Z. Sun, X. H. Chen, *Phys. Rev. B* **2016**, *93*, 060505(R).
[49] D. F. Liu, W. H. Zhang, D. X. Mou, J. F. He, Y. B. Ou, Q. Y. Wang, Z. Li, L. L. Wang, L. Zhao, S. L. He, Y. Y. Peng, X. Liu, C. Y. Chen, L. Yu, G. D. Liu, X. L. Dong, J. Zhang, C. T. Chen, Z. Y. Xu, J. P. Hu, X. Chen, X. C. Ma, Q. K. Xue, X. J. Zhou, *Nat. Commun.* **2012**, *3*, 931.
[50] S. L. He, J. F. He, W. H. Zhang, L. Zhao, D. F. Liu, X. Liu, D. X. Mou, Y. B. Ou, Q. Y. Wang, Z. Li, L. L. Wang, Y. Y. Peng, Y. Liu, C. Y. Chen, L. Yu, G. D. Liu, X. L. Dong, J. Zhang, C. T. Chen, Z. Y. Xu, X. Chen, X. Ma, Q. K. Xue, X. J. Zhou, *Nat. Mater.* **2013**, *12*, 605.
[51] S. Y. Tan, Y. Zhang, M. Xia, Z. R. Ye, F. Chen, X. Xie, R. Peng, D. F. Xu, Q. Fan, H. C. Xu, J. Jiang, T. Zhang, X. C. Lai, T. Xiang, J. P. Hu, B. P. Xie, D. L. Feng, *Nat. Mater.* **2013**, *12*, 634.
[52] Y. Sun, W. H. Zhang, Y. Xing, F. S. Li, Y. F. Zhao, Z. C. Xia, L. L. Wang, X. C. Ma, Q. K. Xue, J. Wang, *Sci. Rep.* **2014**, *4*, 6040.
[53] W. H. Zhang, Y. Sun, J. S. Zhang, F. S. Li, M. H. Guo, Y. F. Zhao, H. M. Zhang, J. P. Peng, Y. Xing, H. C. Wang, T. Fujita, A. Hirata, Z. Li, H. Ding, C. J. Tang, M. Wang, Q. Y. Wang, K. He, S. H. Ji, X. Chen, J. F. Wang, Z. C. Xia, L. Li, Y. Y. Wang, J. Wang, L. L. Wang, M. W. Chen, Q. K. Xue, X. C. Ma, *Chin. Phys. Lett.* **2014**, *31*, 017401.
[54] J.-F. Ge, Z.-L. Liu, C. Liu, C.-L. Gao, D. Qian, Q.-K. Xue, Y. Liu, J.-F. Jia, *Nat. Mater.* **2015**, *14*, 285.
[55] T. Hatakeda, T. Noji, T. Kawamata, M. Kato, Y. Koike, *J. Phys. Soc. Jpn.* **2013**, *82*, 123705.

